Impact of different image reconstructions on PET quantification in non-small cell lung cancer: a comparison of adenocarcinoma and squamous cell carcinoma

Messerli, Michael ; Kotasidis, Fotis ; Burger, Irene A ; Ferraro, Daniela A ; Muehlematter, Urs J ; Weyermann, Corina ; Kenkel, David ; von Schulthess, Gustav K ; Kaufmann, Philipp A ; Huellner, Martin W

Abstract: OBJECTIVE: Positron emission tomography (PET) using 18F-fluordeoxyglucose (F-FDG) is an established imaging modality for tumor staging in patients with non-small cell lung cancer (NSCLC). There is a growing interest in using F-FDG PET for therapy response assessment in NSCLC which relies on quantitative PET parameters such as standardized uptake values (SUV). Different reconstruction algorithms in PET may affect SUV. We sought to determine the variation of SUV in patients with NSCLC when using ordered subset expectation maximization (OSEM) and block sequential regularized expectation maximization (BSREM) in latest-generation digital PET/CT, including a subanalysis for adenocarcinoma and squamous cell carcinoma. METHODS: A total of 58 patients (34 = adenocarcinoma, 24 = squamous cell carcinoma) that underwent a clinically indicated F-FDG PET/CT for staging were reviewed. PET images were reconstructed with OSEM and BSREM reconstruction with noise penalty strength -levels of 350, 450, 600, 800 and 1200. Lung tumors maximum standardized uptake value (SUV) were compared. RESULTS: Lung tumors SUV were significantly lower in adenocarcinomas compared to squamous cell carcinomas in all reconstructions evaluated (all $p < 0.01$). Comparing BSREM to OSEM, absolute SUV differences were highest in lower -levels of BSREM with + 2.9 ± 1.6 in adenocarcinoma and + 4.0 ± 2.9 in squamous cell carcinoma, (difference between histology; p-values > 0.05). There was a statistically significant difference of the relative increase of SUV in adenocarcinoma (mean + 34.8%) and squamous cell carcinoma (mean 23.4%), when using BSREM instead of OSEM ($p < 0.05$). CONCLUSIONS: In NSCLC the relative change of SUV when using BSREM instead of OSEM is significantly higher in adenocarcinoma as compared to squamous cell carcinoma. ADVANCES IN KNOWLEDGE: The impact of BSREM on SUV may vary in different histological subtypes of NSCLC. This highlights the importance for careful standardisation of -value used for serial F-FDG PET scans when following-up NSCLC patients.

DOI: https://doi.org/10.1259/bjr.20180792

(2019). Impact of different image reconstructions on PET quantification in non-small cell lung cancer: a comparison of adenocarcinoma and squamous cell carcinoma. British Journal of Radiology, 92(1096):20180792.
DOI: https://doi.org/10.1259/bjr.20180792

BJR

https://doi.org/10.1259/bjr.20180792

Received: 12 September 2018 | Revised: 05 January 2019 | Accepted: 17 January 2019

Cite this article as:
Messerli M, Kotasidis F, Burger IA, Ferraro DA, Muehlematter UJ, Weyermann C, et al. Impact of different image reconstructions on PET quantification in non-small cell lung cancer: a comparison of adenocarcinoma and squamous cell carcinoma. *Br J Radiol* 2019; **92**: 20180792.

FULL PAPER

Impact of different image reconstructions on PET quantification in non-small cell lung cancer: a comparison of adenocarcinoma and squamous cell carcinoma

[1]MICHAEL MESSERLI, MD, [2]FOTIS KOTASIDIS, PhD, [1]IRENE A. BURGER, MD, [1]DANIELA A. FERRARO, MD, [1,3]URS J. MUEHLEMATTER, MD, [1]CORINA WEYERMANN, MTRA, [1,3]DAVID KENKEL, MD, [1]GUSTAV K. VON SCHULTHESS, MD, PhD, [1]PHILIPP A. KAUFMANN, MD and [1]MARTIN W. HUELLNER, MD

[1]Department of Nuclear Medicine, University Hospital Zurich / University of Zurich, Switzerland
[2]GE Healthcare, Waukesha, WI, USA
[3]Institute of Diagnostic and Interventional Radiology, University Hospital Zurich / University of Zurich, Switzerland

Address correspondence to: Michael Messerli
E-mail: *michael.messerli@usz.ch*

Objective: Positron emission tomography (PET) using ^{18}F-fludeoxyglucose (^{18}F-FDG) is an established imaging modality for tumor staging in patients with non-small cell lung cancer (NSCLC). There is a growing interest in using ^{18}F-FDG PET for therapy response assessment in NSCLC which relies on quantitative PET parameters such as standardized uptake values (SUV). Different reconstruction algorithms in PET may affect SUV. We sought to determine the variation of SUV in patients with NSCLC when using ordered subset expectation maximization (OSEM) and block sequential regularized expectation maximization (BSREM) in latest-generation digital PET/CT, including a subanalysis for adenocarcinoma and squamous cell carcinoma.

Methods: A total of 58 patients (34 = adenocarcinoma, 24 = squamous cell carcinoma) who underwent a clinically indicated ^{18}F-FDG PET/CT for staging were reviewed. PET images were reconstructed with OSEM and BSREM reconstruction with noise penalty strength β-levels of 350, 450, 600, 800 and 1200. Lung tumors maximum standardized uptake value (SUV_{max}) were compared.

Results: Lung tumors SUV_{max} were significantly lower in adenocarcinomas compared to squamous cell carcinomas in all reconstructions evaluated (all $p < 0.01$). Comparing BSREM to OSEM, absolute SUV_{max} differences were highest in lower β-levels of BSREM with + 2.9 ± 1.6 in adenocarcinoma and + 4.0 ± 2.9 in squamous cell carcinoma (difference between histology; p-values > 0.05). There was a statistically significant difference of the relative increase of SUV_{max} in adenocarcinoma (mean + 34.8%) and squamous cell carcinoma (mean 23.4%), when using $BSREM_{350}$ instead of $OSEM_{TOF}$ ($p < 0.05$).

Conclusion: In NSCLC the relative change of SUV when using BSREM instead of OSEM is significantly higher in adenocarcinoma as compared to squamous cell carcinoma.

Advances in knowledge: The impact of BSREM on SUV may vary in different histological subtypes of NSCLC. This highlights the importance for careful standardization of β-value used for serial ^{18}F-FDG PET scans when following-up NSCLC patients.

INTRODUCTION

Non-small cell lung cancer (NSCLC) is the most common cause of mortality from cancer worldwide.[1] In NSCLC, positron emission tomography (PET) using ^{18}F-fludeoxyglucose (^{18}F-FDG) as radiotracer in combination with CT is the established imaging modality for whole-body staging.[2] The high correlation between maximum standardized uptake values (SUV_{max}) of ^{18}F-FDG PET/CT with histopathological tumor regression on radiotherapy[3] as well as neoadjuvant chemotherapy[4] in NSCLC patients lead to an increasing use of ^{18}F-FDG PET for treatment response assessment.[5] However, response assessment with absolute quantitative methods for ^{18}F-FDG PET/CT requires a fundamental standardization and global consensus on imaging protocols and post-processing. Therefore, relative changes have been established to compare response

rates of tumors.[6,7] Still this relative assessment warrants careful standardization of ^{18}F-FDG PET/CT protocol within each institution, especially if used in multicenter trials, as otherwise the inherent value of quantitative PET may be lost.[8] Besides the recommended control of blood glucose levels, standardized uptake time (60 min, range 55–75 min) and ^{18}F-FDG dosage (MBq/kg), also image reconstruction is listed as an important factor for standardizing PET acquisition in order to provide reliable and reproducible quantification.[9]

In current clinical routine, ordered subset expectation maximization (OSEM) reconstruction is the most widely used algorithm for clinical PET/CT as it provides better image quality than the formerly used filtered back projection method.[10] However, it is known that regardless of the reconstruction method used, PET generally underestimates the true SUV as a measure of tumor glucose metabolism.[11] However, previous studies reported that newly clinically available Bayesian penalized likelihood (BPL) reconstruction algorithms such as block sequential regularized expectation maximization (BSREM) may increase the accuracy of lesion quantitation compared to OSEM (*i.e.* lead to an increase of SUV of metabolic active lung lesions).[12] Meanwhile, the variation of PET SUVs due to different reconstruction methods introduces some uncertainties when used for response assessment in NSCLC. It is not understood, if such SUV inconsistencies among different reconstruction may be clinically relevant or not.

Accordingly, we sought to determine the absolute and relative variation of SUV comparing OSEM and BSREM on a latest-generation digital PET/CT in patients with NSCLC, including subanalyses for adenocarcinoma and squamous cell carcinoma.

METHODS AND MATERIALS

Patient selection

Patients undergoing a clinically indicated ^{18}F-FDG PET/CT scan between March 2017 and July 2018 were retrospectively included if they met the following inclusion criteria: (a) patients NSCLC referred for initial staging, (b) histologically confirmed adenocarcinoma or squamous cell carcinoma, (c) written informed consent for the subsequent use of medical data. A part of the study group was shared in a previous publication on another purpose than the present study. The study was approved by the local ethics committee. The study was conducted in compliance with ICH-GCP-rules and the Declaration of Helsinki.

PET/CT acquisition

All patients underwent a PET/CT on a novel digital detector scanner (GE Discovery Molecular Insights—DMI PET/CT, GE Healthcare, Waukesha, WI). A body mass index (BMI) adapted ^{18}F-FDG dosage protocol was used, based on recommendations for this specific digital PET detector[13]: a dose of 1.5 MBq per kilogram body weight was injected for patients with a BMI of <20 kg m^{-2}, 2 MBq per kilogram body weight for patients with a BMI of 20–24.5 kg/m^2, and 3.1 MBq per kilogram body weight for patients with a BMI >24.5 kg/m^{-2}, up to a maximum of 320 MBq. The participants fasted for at least 4 h prior to the scan and blood glucose levels were <160 mg dl^{-1} at the time of ^{18}F-FDG injection. A CT scan was obtained from the vertex to the mid-thighs and used for attenuation correction as well as to help for anatomic localization of ^{18}F-FDG uptake. The CT was performed with automated dose modulation (range 15–100 mA, 120 kV). After the CT, a PET scan was acquired covering the same anatomical region. The PET acquisition time was 2.5 min per bed position, with 6–8 bed positions per patient (depending on patient size), with an overlap of 23%. For calibration of the PET scanner used in the present study daily quality control is performed with an annulus Ge-68 phantom while well counter calibration for absolute quantification is performed with an F-18 filled phantom.

PET data reconstructions

After PET image acquisition, data sets were reconstructed with seven different reconstruction settings per patient, two reconstructions were using OSEM with two iterations, 24 subsets and 6.4 mm Gaussian filter (1) with time-of-flight (TOF) acquisition ($OSEM_{TOF}$; VUE Point FX, GE Healthcare, Waukesha, WI), (2) with TOF and point spread function (PSF) modelling ($OSEM_{PSF}$; VUE Point FX with SharpIR, GE Healthcare, Waukesha, WI). Five reconstructions used BSREM (Q.Clear, GE Healthcare, Waukesha, WI) with incremental β-values of (3) 350, (4) 450, (5) 600, (6) 800, and (7) 1200. All data sets were reconstructed with a 256 × 256 pixel matrix. The background for choosing this reconstruction settings was as follows: $OSEM_{TOF}$ is frequently used in clinical multicenter studies for the purpose of interscanner and intersite harmonization. $OSEM_{PSF}$ represents the latest reconstruction technique used on many PET/CT systems. BSREM, on the other hand, is a full convergence algorithm that reaches high convergence, which may become a clinical standard in the future, at least for digital scanners.

Quantitative imaging analysis

Quantitative analyses were performed by two readers (D.A.F. and M.M., 3 and 6 years of experience in chest imaging). The SUV_{max} of each primary lung tumor was recorded using a standard volume of interest (VOI) tool including the whole tumor volume. Thereby, the VOI was automatically propagated to cover the exact same volume in all the different reconstruction sets. The cases with discrepancy of lung tumor SUV_{max} between the two readers were noted and resolved in consensus.

Further, as a measure of image noise the standard deviation of the standardized uptake value (SUV_{SD}) in the right lobe of the liver (parenchymal organ background) and within the descending aorta (bloodpool background) at the level of the carina was measured using a 4.0 cm and 1.0 cm diameter spherical VOI, respectively.

Statistical analyses

Categorical variables are expressed as proportions, and continuous variables are presented as mean ± standard deviation or median (range) depending on the distribution of values. Demographics and quantitative PET data were compared between adenocarcinoma and squamous cell carcinoma patients using the Mann–Whitney *U* test or χ^2 test. Intraclass correlation coefficient (ICC) was calculated between each pair of lung tumor SUVmax value to agreement among the two readers. According

to Meyers et al, an ICC <0.69 was defined as poor, ICC between 0.70 and 0.79 as fair, ICC between 0.80 and 0.89 as good and ICC >0.9 as high agreement.[14] Further, we assessed the frequency of SUV-changes that were >30% or <30% comparing BSREM with OSEM, separately for adenocarcinoma and squamous cell carcinoma. The 30% cutoff was chosen corresponding to similar requirements for SUV change to address tumor response in other studies and guidelines.[6] Analyses were carried out using SPSS release 23.0 (IBM Corporation, Armonk, NY) and MedCalc v. 18.2 (MedCalc Software, Ostend, Belgium). A two-tailed p-value of <0.05 was considered to indicate statistical significance.

RESULTS

A total of 58 patients (23 female, 35 male; median age 67, range 46–83 years) referred for initial staging with ^{18}F-FDG PET/CT were included in this study. The patients had histologically confirmed adenocarcinoma (n = 34) and squamous cell carcinoma (n = 24). Further demographic information on study patients is given in Table 1.

SUV_{max} in adenocarcinoma and squamous cell carcinoma

ICC indicated high agreement of lung tumor SUV_{max} measurements among the two readers with 0.951 [$p < 0.001$, 95% confidence interval (CI) 0.919–0.971]. A total of four (7%) cases with discrepancy of SUV measurements were resolved in consensus. The results of the quantitative assessment including all study patients are given in Table 2 and Figure 1. SUV_{max} was significantly lower in adenocarcinomas compared to squamous cell carcinomas in $OSEM_{TOF}$ and $OSEM_{PSF}$ as well as in all BSREM reconstructions (all $p < 0.01$). $BSREM_{350}$ resulted in the highest SUV_{max} for primary lung tumors with an average of 12.0 ± 5.0 in adenocarcinoma and 18.1 ± 9.3 in squamous cell carcinoma, whereas we observed the lowest SUV_{max} in $OSEM_{TOF}$ with a SUV_{max} of 9.2 ± 4.0 in adenocarcinoma and 14.5 ± 7.0 in squamous cell carcinoma, respectively.

Absolute and relative differences of PET values in different NSCLC histology

Table 3 demonstrates absolute and relative SUV_{max} differences of primary lung tumors among OSEM and BSREM reconstructions in adenocarcinoma and squamous cell carcinoma. Comparing BSREM to $OSEM_{TOF}$, absolute SUV_{max} differences were highest in lower BSREM levels of 350 in adenocarcinoma with +2.9 ± 1.6 and in squamous cell carcinoma with +4.0 ± 2.9, respectively. Absolute differences of SUV_{max} in reconstruction were similar in adenocarcinoma and squamous cell carcinoma (all p-values > 0.05).

We observed a statistically significant difference of the relative increase of SUV_{max} in adenocarcinoma compared to squamous cell carcinoma in $BSREM_{350}$ compared to $OSEM_{TOF}$, $BSREM_{350}$ compared to $OSEM_{PSF}$, and $BSREM_{450}$ compared to $OSEM_{PSF}$, respectively (Table 3).

Image noise (*i.e.,* SUV_{SD}) in the bloodpool and the liver using OSEM and BSREM reconstructions were similar comparing PET scans of patients with adenocarcinoma and squamous cell carcinoma (all p-values > 0.05), see Table 3.

Representative images of study subjects undergoing ^{18}F-FDG PET/CT for lung cancer staging are given in Figure 2.

Impact of reconstruction methods on clinical tumor response assessment

We observed a significantly higher frequency of tumors that showed an increase of SUV_{max} >30% with BSREM compared to $OSEM_{TOF}$ in patients with adenocarcinoma (up to 56% of patients) compared to patients with squamous cell carcinoma (up to 29% of patients)(Figure 3). This was also observed, but less pronounced, when comparing BSREM with $OSEM_{PSF}$ (see Figure 3).

DISCUSSION

This study sought to investigate if the impact of different reconstruction algorithms (OSEM and BSREM) on absolute and relative SUV using digital PET/CT in lung cancer patients is clinically relevant. The major findings of our study are as follows: (1) the absolute increase of SUV_{max} when applying BSREM instead of OSEM is not significantly different among adenocarcinoma and squamous cell carcinoma, (2) the mean relative increase of SUV_{max} comparing $BSREM_{350}$ with $OSEM_{TOF}$ is +34.8% in adenocarcinoma and 23.4% in squamous cell carcinoma, (3) the relative increase of SUV comparing BSREM with OSEM may be significantly different among different histological subtypes of NSCLC, and (4) compared with OSEM the use of BSREM may increase the SUV_{max} of lung tumor by >30% in up to 56% of cases in adenocarcinoma and 25% of squamous cell carcinoma.

There is an increasing interest in quantitative ^{18}F-FDG PET/CT as a tool for diagnosis, estimation of prognosis, and response monitoring in oncological diseases. If absolute quantification of metabolism by PET is achieved and results in consistent numerical values of such, between different scanners and institutes that acquire the scans this would further enhance the role of this modality as an invaluable tool, particularly for therapy response assessment. However, PET/CT quantification using, SUV may be affected by different physiological and several technical factors,[9] including different reconstruction methods.[11,12] As a consequence, some of the variations in the literature on SUV-based patient outcomes may be explained by differences in ^{18}F-FDG PET/CT study methods. With regard to NSCLC, former analysis suggested differences in the expression of proteins for glucose metabolism (*e.g.* GLUT1-transporter) between its two most frequent histological subtypes; adenocarcinoma and squamous cell carcinoma.[15] This may explain the fact that there are variations of ^{18}F-FDG uptake in different tumor histology with adenocarcinomas generally showing lower ^{18}F-FDG uptake compared to squamous cell carcinomas.[16,17] Indeed, also in our study group we observed significantly different SUV_{max} among different NSCLC histological subtypes, regardless of the reconstruction method used, *e.g.* with a higher average SUV_{max} of 14.5 (range 2.9–36.2) in squamous cell carcinomas as compared to 9.2 (range 2.3–17.1) in adenocarcinoma using $OSEM_{TOF}$.

Table 1. Demographic data of study subjects (n = 58)

	Adenocarcinoma, n = 34	**Squamous cell carcinoma, n = 24**	**p-value[a]**
Female/male, n (%)	18 (53%)/16 (47%)	5 (21%)/19 (79%)	0.015
Age, years, median (range)	66 (46–82)	70 (51–83)	0.076
Body weight, kg	71 ± 21 (39–124)	73 ± 14 (46–114)	0.421
Body height, m	1.70 ± 0.1 (1.49–1.87)	1.73 ± 0.1 (1.59–1.86)	0.343
BMI, kg/m^2	24.3 ± 5.5 (15.0–38.7)	24.4 ± 4.2 (16.9–36.8)	0.608
Blood glucose level, mg/dl	100 ± 15 (72–157)	104 ± 20 (79–169)	0.434
Injected tracer activity, MBq	176 ± 79 (85–318)	180 ± 69 (91–295)	0.636
Scan time post-injection, min	60 ± 6 (50–76)	64 ± 11 (54–97)	0.141
PET/CT performed			0.898
After histology	26 (76%)	18 (75%)	
Before histology	8 (24%)	6 (25%)	
Time period scan after biopsy, d	16 ± 16 (1–57)	16 ± 12 (1–46)	0.452
Time period scan before biopsy, d	11 ± 6 (2–22)	31 ± 41 (2–104)	0.897
Maximal tumor diameter on CT, cm	4.3 ± 1.9 (1.7–8.4)	5.1 ± 2.2 (1.5–9.5)	0.155
T-classification			0.236
T1	9 (26%)	3 (13%)	
T2	9 (26%)	11 (46%)	
T3	7 (21%)	3 (13%)	
T4	9 (26%)	7 (29%)	
N-classification			0.056
N0	11 (32%)	8 (33%)	
N1	6 (18%)	5 (21%)	
N2	7 (21%)	5 (21%)	
N3	10 (29%)	6 (25%)	
M-classification			0.386
M0	14 (41%)	20 (83%)	
M1	20 (59%)	4 (17%)	
UICC stage, n (%)			0.408
I	4 (12%)	3 (13%)	
II	3 (9%)	7 (29%)	
III	7 (21%)	10 (42%)	
IV	20 (59%)	4 (17%)	

CT = computed tomography; MBq = Mega Becquerel; PET = Positron emission tomography; BMI, body mass index.
Values are given as absolute numbers and percentages in parenthesis or mean ± standard deviation (range) if not stated otherwise.
[a]χ^2 test and Mann–Whitney U test for non-paired non-parametric data.

In recent years, OSEM reconstructions have been widely used instead of the initially used filtered back projection because of their overall improvement of image quality.[18,19] OSEM methods thereby repeatedly iterate different possibilities of the raw data to find the most likely image and with each iteration step an image with a greater likelihood of describing the measured data is achieved. The main disadvantage of OSEM, however, is that it is not possible to run it to full convergence as the noise of PET images increases with each iteration step, leading to somewhat unacceptable images before full convergence is reached.[11,20] Therefore, OSEM is stopped after a predefined number of iterations, resulting in underconverged images. As stated before, this leads to an underestimation of PET values, such as SUV. In contrast, novel BPL methods incorporate a penalty function (*i.e.* the β-value) as the only user-input variable which allows to choose the level of noise suppression applied and enables

Table 2. SUV_{max} of the primary lung tumor in different reconstruction settings as well as standard deviation of the standardized uptake value (SUV_{SD}) as a measure for image noise

		OSEM		BSREM				
		$OSEM_{TOF}$	$OSEM_{PSF}$	$BSREM_{350}$	$BSREM_{450}$	$BSREM_{600}$	$BSREM_{800}$	$BSREM_{1200}$
Adenocarcinoma, $n = 34$	SUV_{max}							
	Mean	9.2	9.8	12.0	11.5	11.0	10.5	10.0
	Median	9.2	9.8	11.8	11.4	11.8	10.4	9.9
	Range	2.3–17.1	2.3–18.7	2.6–24.4	2.5–23.8	2.5–22.9	2.4–21.9	2.3–20.2
Squamous cell carcinoma, $n = 24$	SUV_{max}							
	Mean	14.5	15.5	18.1	17.5	17.0	16.4	15.6
	Median	14.0	14.6	16.9	16.3	15.6	15.1	14.7
	Range	2.9–36.2	3.2–39.3	3.7–49.7	3.6–48.0	3.4–46.0	3.2–43.8	2.9–40.5
p-value[a]		0.001	0.001	0.005	0.004	0.003	0.002	0.001
Adenocarcinoma, $n = 34$	Image noise[b]							
	Mediastinum	0.15 ± 0.05	0.13 ± 0.05	0.18 ± 0.05	0.14 ± 0.04	0.12 ± 0.03	0.10 ± 0.02	0.08 ± 0.02
	Liver	0.28 ± 0.07	0.25 ± 0.06	0.30 ± 0.06	0.26 ± 0.05	0.22 ± 0.04	0.19 ± 0.04	0.15 ± 0.03
Squamous cell carcinoma, $n = 24$	Image noise[b]							
	Mediastinum	0.16 ± 0.07	0.14 ± 0.06	0.19 ± 0.09	0.16 ± 0.08	0.13 ± 0.06	0.11 ± 0.05	0.09 ± 0.04
	Liver	0.28 ± 0.07	0.26 ± 0.07	0.29 ± 0.07	0.26 ± 0.06	0.22 ± 0.06	0.19 ± 0.05	0.16 ± 0.04
p-value[a]	Mediastinum	0.752	0.856	0.807	0.812	0.733	0.962	0.589
p-value[a]	Liver	0.899	0.931	0.472	0.602	0.862	0.681	0.937

BSREM, block sequential regularized expectation maximization; OSEM, ordered subset expectation maximization; PSF, point spread function modelling; SUV_{max}, maximum standardized uptake value; TOF, time of flight.

p-values for comparison of SUVs in adenocarcinomas and squamous cell carcinomas are given at the bottom of the table.

[a]Mann–Whitney *U* test

[b]SUV_{SD}; measured in a 1.0 cm spherical VOI in the descending aorta and a 4.0 cm spherical VOI in the right lobe of the liver

Figure 1. Box plots of absolute SUV_{max} for all primary lung tumors for OSEM and BSREM reconstruction, for patients with adenocarcinoma (n = 34) and squamous cell carcinoma (n = 24). Box and whisker plots show IQR from the 25 to 75% percentile and the upper fence of the 1.5 IQR above the 75% percentile or lower fence of the 1.5 IQR below the 25% percentile. * $p < 0.01$; ** $p = 0.001$; for SUV_{max} in squamous cell carcinoma compared to adenocarcinoma. BSREM, block sequential regularized expectation maximization; OSEM, ordered subsetexpectation maximization; IQR, interquartile range.

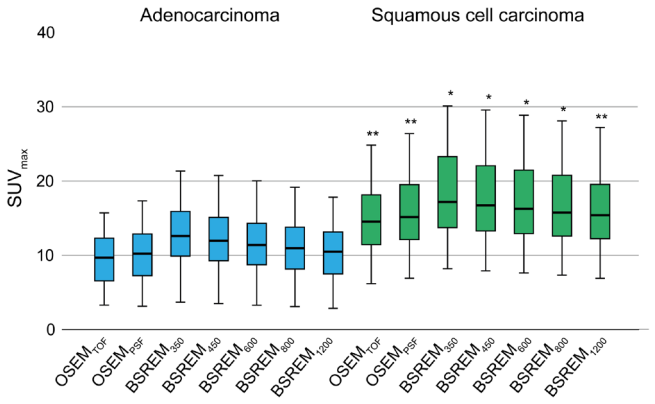

to increase the number of iterations without excessive image noise.[21] BSREM is an algorithm that is used to solve this penalized likelihood objective function. Thereby, it can use more iterations without recovering high frequency components from noise. Hence, it can get very close to convergence at the voxel level and it was already previously described that BPL-based reconstruction may increase the accuracy of lesion quantitation compared to OSEM, with a particular improvement in quantification in cold background regions such as the lungs.[22]

An attempt to explain the principal finding of why relative SUV changes in digital PET/CT using BSREM instead of OSEM are significantly different among different NSCLC histologies may be as follows: given the usually lower SUV of adenocarcinomas, as aforementioned, they are more underconverged using OSEM reconstruction compared to squamous cell carcinoma. This can be attributed to the fact that one has a higher activity concentration to the other on average, hence it is known that focal uptake with higher activity concentration tend to converge faster and uptake with lower activity concentration tend to converge slower. So the convergence benefit of BSREM reconstruction in providing more convergent foci compared to OSEM is more felt with adenocarcinoma as they are more underconverged and have a differential improvement to squamous cell carcinoma.

Table 3. Absolute and relative SUV_{max} differences among OSEM and BSREM reconstructions of lung cancers

		Adenocarcinoma, n = 34	Squamous cell carcinoma, n = 24	p-value[a]
Absolute ΔSUV_{max}	$BSREM_{350}$ to $OSEM_{TOF}$	+2.9±1.6	+4.0±2.9	0.403
	$BSREM_{450}$ to $OSEM_{TOF}$	+2.4±1.5	+3.4±2.5	0.324
	$BSREM_{600}$ to $OSEM_{TOF}$	+1.9±1.4	+2.8±2.1	0.132
	$BSREM_{800}$ to $OSEM_{TOF}$	+1.4±1.3	+2.1±1.6	0.029
	$BSREM_{1200}$ to $OSEM_{TOF}$	+0.8±1.0	+1.2±1.0	0.077
Relative ΔSUV_{max}	$BSREM_{350}$ to $OSEM_{TOF}$	+34.8±20.5%	+23.4%±7.7	0.048
	$BSREM_{450}$ to $OSEM_{TOF}$	+28.8±18.4%	+19.7%±6.2	0.072
	$BSREM_{600}$ to $OSEM_{TOF}$	+22.6±16.7%	+16.2%±5.1	0.276
	$BSREM_{800}$ to $OSEM_{TOF}$	+16.2±14.9%	+12.6%±4.2	0.728
	$BSREM_{1200}$ to $OSEM_{TOF}$	+9.7±11.7%	+7.3%±3.4	0.528
Absolute ΔSUV_{max}	$BSREM_{350}$ to $OSEM_{PSF}$	+2.2±1.2	+2.9±2.3	0.788
	$BSREM_{450}$ to $OSEM_{PSF}$	+1.7±1.1	+2.2±1.9	0.597
	$BSREM_{600}$ to $OSEM_{PSF}$	+1.2±1.0	+1.7±1.5	0.269
	$BSREM_{800}$ to $OSEM_{PSF}$	+0.7±0.8	+1.0±1.0	0.136
	$BSREM_{1200}$ to $OSEM_{PSF}$	+0.1±0.7	+0.1±0.5	0.868
Relative ΔSUV_{max}	$BSREM_{350}$ to $OSEM_{PSF}$	+24.4±13.8%	+15.6%±5.6	0.012
	$BSREM_{450}$ to $OSEM_{PSF}$	+18.9±11.7%	+12.1%±4.1	0.021
	$BSREM_{600}$ to $OSEM_{PSF}$	+13.2±10.1%	+8.8%±3.3	0.172
	$BSREM_{800}$ to $OSEM_{PSF}$	+7.3±8.7%	+5.4%±2.7	0.850
	$BSREM_{1200}$ to $OSEM_{PSF}$	+1.4±6.7%	+0.5%±2.7	0.425

BSREM, block sequential regularized expectation maximization; OSEM, ordered subset expectation maximization; PSF, point spread function modelling; SUV_{max}, maximum standardized uptake value; TOF, time of flight.
Values are given as mean ± standard deviation.
[a]Mann–Whitney U test

Figure 2. Representative images of patients that underwent ^{18}F-FDG PET/CT for lung cancer staging. Axial PET/CT images (A, B) show FDG-avid intrapulmonary lesions. Histopathology confirmed an adenocarcinoma in (A) and squamous cell carcinoma in (B). Corresponding SUV_{max} are presented (C and D) for $OSEM_{TOF}$, $OSEM_{PSF}$, $BSREM_{350}$, $BSREM_{450}$, $BSREM_{600}$, $BSREM_{800}$, and $BSREM_{1200}$. While the absolute increase of SUV_{max} using BSREM compared to OSEM is similar in both cases, the relative increase is more pronounced in the patient with adenocarcinoma. ^{18}F-FDG, ^{18}F-fludeoxyglucose; BSREM, block sequential regularized expectation maximization; OSEM, ordered subset expectation maximization; SUV_{max}, maximum standardized uptake value.

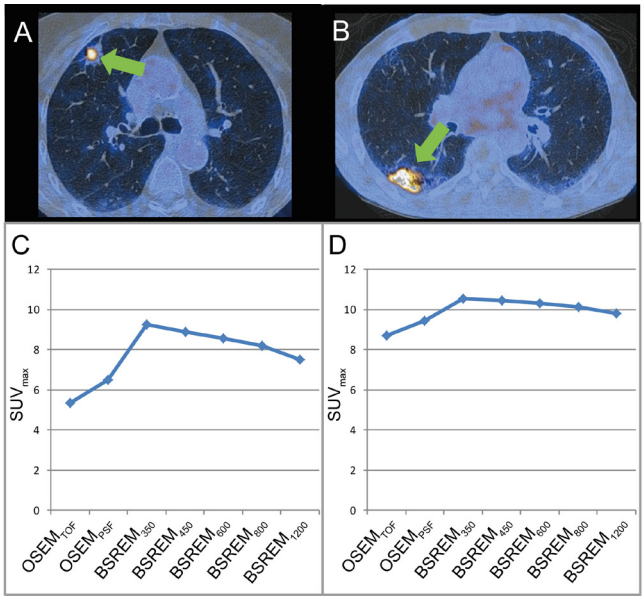

Figure 3. Frequency of patients with an SUV_{max} increase by >30% when using BSREM instead of OSEM. We observed the tumor SUV_{max} to increase by >30% most often in patients with adenocarcinoma, when using BSREM with lower β-values, and when comparing BSREM with $OSEM_{TOF}$ (A). This was less frequent when comparing BSREM with $OSEM_{PSF}$ (B).

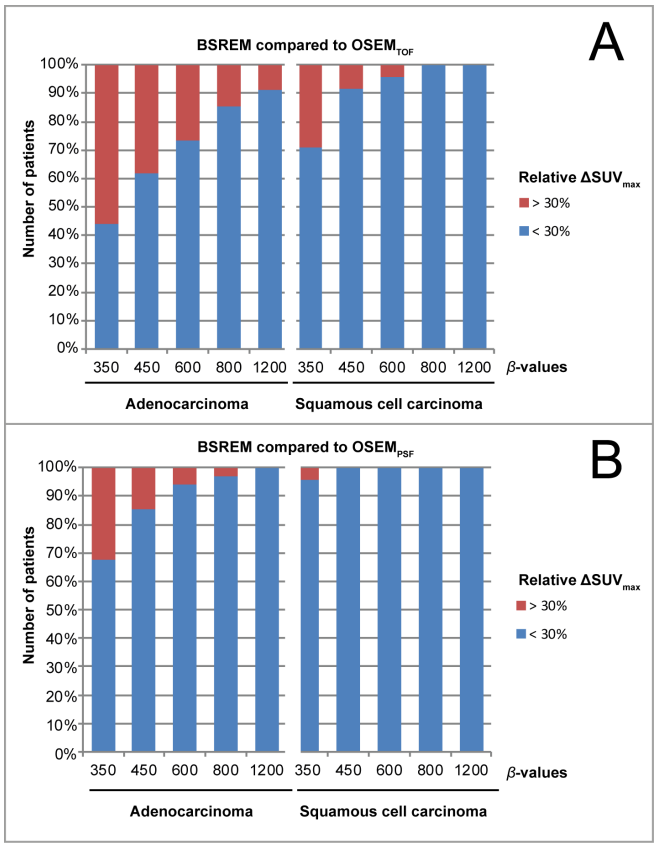

We could argue that the changes we see with BSREM are due to histology differences but also due to the underconvergence difference produced by OSEM which is again less for squamous cell carcinoma. Therefore, the benefit of convergence with BSREM is more pronounced with adenocarcinoma. This also leads to the fact that differences with BSREM are more indicative of real histology difference than differences occurring from differential convergence of OSEM. One might also extrapolate this to other subtypes of cancers since this effect is reconstruction-related. Future studies may have to elucidate absolute and relative impact of BSREM compared to OSEM as well.

Overall, this fact needs to be taken into account if SUV are used as a basis for treatment strategy decisions or outcome comparisons across different centers. We even observed a substantial number of patients (up to 56%) that had an increase of lung tumor SUV_{max} by >30% simply by using BSREM instead of OSEM. This was more often observed in adenocarcinomas than in squamous cell carcinomas. Notably, such increases were particularly seen with lower β-values (19/34 adenocarcinomas with $BSREM_{350}$, 13/34 with $BSREM_{450}$). In another study, such low β-values were shown to yield the optimum image quality for lung cancer,[23] and are hence expected to be utilized more frequently in the staging of lung cancer patients compared to reconstruction settings with higher β-values. A recent study by Furumoto et al investigated the predictive value of PET/CT in clinical stage IA adenocarcinomas of the lung in terms of clinical outcome and pathological invasiveness.[24] Notably, Furumoto et al found that aside the volume of the solid part of the pulmonary lesion, the SUV_{max} (cutoff value of 2.4 using OSEM) was highly beneficial for the prediction of survival and pathological invasiveness. This study is exemplary for the raising prognostic importance of ^{18}F-FDG PET/CT. Relating their results to the results of our study, we assume that these cutoff values would need to be adapted when using BSREM instead of OSEM. Further studies may elucidate SUV adaptions needed for different tumor entities, tumor histologies and clinical scenarios when applying BSREM.

There are some limitations of our study that have to be considered. First, the included number of patients is relatively small and only from a single center, therefore further studies, ideally in a multicenter setting, are needed to confirm our findings. Second, analyses of tumor SUV were restricted to measurement of SUV_{max}, which remains the main parameter used in clinical care. Future evaluations of corrected SUV-values may lead to different results for different reconstruction methods. Third, given that more patients with NSCLC referred to our department for imaging are diagnosed with adenocarcinoma as compared to

squamous cell carcinoma we were not able to include a 1:1 ratio of this two histological subtypes which may be desired in future evaluations.

CONCLUSIONS

BSREM leads to a significant increase of SUV in both adenocarcinoma and squamous cell carcinoma compared to OSEM. The relative change of SUV_{max} comparing BSREM with OSEM may be significantly different among different histological subtypes of NSCLC and is more pronounced in adenocarcinomas. This highlights the importance for careful standardisation of β-value used for serial ^{18}F-FDG PET scans when following-up NSCLC patients.

ACKNOWLEDGEMENT

Michael Messerli received a research grant from the Iten-Kohaut Foundation, Switzerland. Martin W. Huellner is a recipient of the Alfred and Annemarie von Sick grant for translational and clinical cardiac and oncological research. We thank Josephine Trinckauf, Freya Klein, Kevin Frei and Lasien Vojo for their excellent technical support.

FUNDING

The University Hospital Zurich holds a research agreement with GE Healthcare (unrelated to current study). No further specific grants from funding agencies in the public, commercial, or not-for-profit sectors were received for this study.

CONFLICT OF INTEREST

FK is an employee of GE Healthcare. GKvS is a Consultant to GE Healthcare and a Co-Director of IDKD, an educational organization which receives funds from multiple companies. MM, IAB and MWH received speaker's fees from GE Healthcare. Apart from that, the other authors of this manuscript declare no relationships with any companies, whose products or services may be related to the subject matter of the article. The University Hospital Zurich holds a research agreement with GE Healthcare. Only non-GE employees had control of inclusion of data and information that might present a conflict of interest for those authors who are employees of GE Healthcare.

REFERENCES

1. Stewart B, Wild C. World cancer report 2012. *International Agency for Research on Cancer* 2014.
2. Lardinois D, Weder W, Hany TF, Kamel EM, Korom S, Seifert B, et al. Staging of non-small-cell lung cancer with integrated positron-emission tomography and computed tomography. *N Engl J Med* 2003; **348**: 2500–7. doi: https://doi.org/10.1056/NEJMoa022136
3. Mac Manus MP, Hicks RJ, Matthews JP, McKenzie A, Rischin D, Salminen EK, et al. Positron emission tomography is superior to computed tomography scanning for response-assessment after radical radiotherapy or chemoradiotherapy in patients with non-small-cell lung cancer. *J Clin Oncol* 2003; **21**: 1285–92. doi: https://doi.org/10.1200/JCO.2003.07.054
4. Nahmias C, Hanna WT, Wahl LM, Long MJ, Hubner KF, Townsend DW. Time course of early response to chemotherapy in non-small cell lung cancer patients with 18F-FDG PET/CT. *J Nucl Med* 2007; **48**: 744–51. doi: https://doi.org/10.2967/jnumed.106.038513
5. Michaelis LC, Ratain MJ. Measuring response in a post-RECIST world: from black and white to shades of grey. *Nat Rev Cancer* 2006; **6**: 409–14. doi: https://doi.org/10.1038/nrc1883
6. Wahl RL, Jacene H, Kasamon Y, Lodge MA. From RECIST to PERCIST: evolving considerations for PET response criteria in solid tumors. *J Nucl Med* 2009; **50**(Suppl 1): 122S–50. doi: https://doi.org/10.2967/jnumed.108.057307
7. Young H, Baum R, Cremerius U, Herholz K, Hoekstra O, Lammertsma AA, et al. Measurement of clinical and subclinical tumour response using [18F]-fluorodeoxyglucose and positron emission tomography: review and 1999 EORTC recommendations. European Organization for Research and Treatment of Cancer (EORTC) PET Study Group. *Eur J Cancer* 1999; **35**: 1773–82.
8. Boellaard R, Delgado-Bolton R, Oyen WJ, Giammarile F, Tatsch K, Eschner W, et al. FDG PET/CT: EANM procedure guidelines for tumour imaging: version 2.0. *Eur J Nucl Med Mol Imaging* 2015; **42**: 328–54. doi: https://doi.org/10.1007/s00259-014-2961-x
9. Boellaard R. Standards for PET image acquisition and quantitative data analysis. *J Nucl Med* 2009; **50**(Suppl 1): 11S–20. doi: https://doi.org/10.2967/jnumed.108.057182
10. Tsoumpas C, Turkheimer FE, Thielemans K. Study of direct and indirect parametric estimation methods of linear models in dynamic positron emission tomography. *Med Phys* 2008; **35**: 1299–309. doi: https://doi.org/10.1118/1.2885369
11. Adams MC, Turkington TG, Wilson JM, Wong TZ. A systematic review of the factors affecting accuracy of SUV measurements. *AJR Am J Roentgenol* 2010; **195**: 310–20. doi: https://doi.org/10.2214/AJR.10.4923
12. Teoh EJ, McGowan DR, Bradley KM, Belcher E, Black E, Gleeson FV. Novel penalised likelihood reconstruction of PET in the assessment of histologically verified small pulmonary nodules. *Eur Radiol* 2016; **26**: 576–84. doi: https://doi.org/10.1007/s00330-015-3832-y
13. Sekine T, Delso G, Zeimpekis KG, de Galiza Barbosa F, Ter Voert E, Huellner M, et al. Reduction of ^{18}F-FDG Dose in Clinical PET/MR Imaging by Using Silicon Photomultiplier Detectors. *Radiology* 2018; **286**: 249–59. doi: https://doi.org/10.1148/radiol.2017162305
14. Meyers CR, Blesh TE. *Measurement in physical education*. New York: Ronald Press; 1962.
15. Meijer TW, Schuurbiers OC, Kaanders JH, Looijen-Salamon MG, de Geus-Oei LF, Verhagen AF, et al. Differences in metabolism between adeno- and squamous cell non-small cell lung carcinomas: spatial distribution and prognostic value of GLUT1 and MCT4. *Lung Cancer* 2012; **76**: 316–23. doi: https://doi.org/10.1016/j.lungcan.2011.11.006
16. Schuurbiers OC, Meijer TW, Kaanders JH, Looijen-Salamon MG, de Geus-Oei LF, van der Drift MA, et al. Glucose metabolism in NSCLC is histology-specific and diverges the prognostic potential of 18FDG-PET for adenocarcinoma and squamous cell carcinoma. *J Thorac Oncol* 2014; **9**:

1485–93. doi: https://doi.org/10.1097/JTO.0000000000000286
17. Tsutani Y, Miyata Y, Misumi K, Ikeda T, Mimura T, Hihara J, et al. Difference in prognostic significance of maximum standardized uptake value on [18F]-fluoro-2-deoxyglucose positron emission tomography between adenocarcinoma and squamous cell carcinoma of the lung. *Jpn J Clin Oncol* 2011; **41**: 890–6. doi: https://doi.org/10.1093/jjco/hyr062
18. Akamatsu G, Ishikawa K, Mitsumoto K, Taniguchi T, Ohya N, Baba S, et al. Improvement in PET/CT image quality with a combination of point-spread function and time-of-flight in relation to reconstruction parameters. *J Nucl Med* 2012; **53**: 1716–22. doi: https://doi.org/10.2967/jnumed.112.103861
19. Boellaard R, van Lingen A, Lammertsma AA. Experimental and clinical evaluation of iterative reconstruction (OSEM) in dynamic PET: quantitative characteristics and effects on kinetic modeling. *J Nucl Med* 2001; **42**: 808–17.
20. Tong S, Alessio AM, Kinahan PE. Image reconstruction for PET/CT scanners: past achievements and future challenges. *Imaging Med* 2010; **2**: 529–45. doi: https://doi.org/10.2217/iim.10.49
21. Ross S. Q.clear (GE healthcare white paper). 2013. Available from: http://www3gehealthcarecom/~/media/documents/us-global/products/pet-ct/whitepaper/q%20clear/ge-healthcare-white-paper_qclearpdf [16 December 2017].
22. Ahn S, Ross SG, Asma E, Miao J, Jin X, Cheng L, et al. Quantitative comparison of OSEM and penalized likelihood image reconstruction using relative difference penalties for clinical PET. *Phys Med Biol* 2015; **60**: 5733–51. doi: https://doi.org/10.1088/0031-9155/60/15/5733
23. Messerli M, Stolzmann P, Egger-Sigg M, Trinckauf J, D'Aguanno S, Burger IA, et al. Impact of a Bayesian penalized likelihood reconstruction algorithm on image quality in novel digital PET/CT: clinical implications for the assessment of lung tumors. *EJNMMI Phys* 2018; **5**: 27. doi: https://doi.org/10.1186/s40658-018-0223-x
24. Furumoto H, Shimada Y, Imai K, Maehara S, Maeda J, Hagiwara M, et al. Prognostic impact of the integration of volumetric quantification of the solid part of the tumor on 3DCT and FDG-PET imaging in clinical stage Ia adenocarcinoma of the lung. *Lung Cancer* 2018; **121**: 91–6. doi: https://doi.org/10.1016/j.lungcan.2018.05.001